ACS Macro Letters

Letter

pubs.acs.org/macroletters

Hierarchical Nanostructures and Self-Assemblies in Smectic-Nematic Liquid Crystalline Diblock Copolymers

Wei Wei, Yu Liu, and Huiming Xiong*

Department of Polymer Science, School of Chemistry and Chemical Engineering, Shanghai Jiao Tong University, Shanghai, People's Republic of China

Supporting Information

ABSTRACT: Coexistence of smectic and nematic orders in 3D curvaceous bicontineous cubic or hexagonal hierarchical structures is observed in a novel class of nanophase separated, flexible double liquid crystalline (LC) diblock copolymers of different molecular weights (MWs) but similar compositions, obtained via sequential anionic polymerization. The diblock copolymer of higher MW exhibits an exceptional order−order transition (OOT) from lamellae (Lam) to hexagonal-packed cylinder (HPC) upon nematic ordering. In contrast, the polymer with lower MW forms a thermodynamically stable, ordered gyroid structure, interwining with LC defects on nanoscale. Delicate balance of collective LC interactions and geometric frustration dictates this unique behavior, which offers a genuine way to fine-tune 2D and 3D complex structures with sub-10 nm feature sizes.

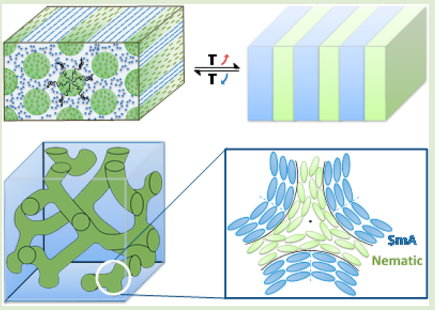

The assembly of atoms, molecules, and larger elements into condensed phases with specific symmetries and spatial dimensions determines the properties of materials. The construction and engineering of structures need manipulation of interfacial curvature and topology.[1] Block copolymer is a fascinating candidate because of their capability of self-assembling into a variety of ordered nanostructures according to the block composition.[2] The past decades have witnessed the development of diverse self-assembly building blocks ranging from crystal,[3,4] liquid crystal[5−12] to supramolecular complex,[13,14] and so on. Among them, LC block copolymers have been extensively studied due to their potential applications in microelectronics, photonics, biology, and nanofabrication processes.[15−18] However, it still remains a challenge to construct sophisticated nanostructures to meet the specific needs of various purposes. For instance, application of block copolymers in the nanolithography techniques calls for 2D and 3D nanostructures with a sub-10 nm feature size.[19−21]

Conventional flexible liquid crystalline diblock copolymers usually produced only three basic structural elements: sphere, cylinder, and lamellae.[2,8] The formation of zero-, one-, and two-dimensional structures is mainly determined by the overall balance of phase separation and geometric restriction in the LC fields. It is more difficult to generate highly curvaceous 3D structures such as an ordered bicontinuous double gyroid (OBDG) structure due to a high elastic energy penalty to distort LC ordering. On another aspect, the feature size of phase separated structure could be potentially reduced via further enhancing the phase incompatibility between the blocks.[8]

In this Letter, we introduce a rational molecular design of block copolymer composed of two prototypical LC phases, namely, smectics and nematics, as an effective strategy to construct a unique class of self-assembling soft material, smectic-nematic (S−N) diblock copolymer. The flexibility of the polyether backbone, mobility and order of the intrinsically immiscible LC phases of distinctly different symmetries,[22] together with microphase separation bring out profound consequences on the phase structure and feature size of the S−N diblock copolymers. Interestingly, two curvaceous structures, uniformly curved cylinder and saddle-shaped gyroid, with feature sizes of sub-10 nm or even sub-5 nm scale have been discovered. The evolution of the structures and the delicate balance between LC order and microphase separation during the self-assembly process have been explicitly revealed.

Two monodisperse S−N diblock copolymers $E_{26}Y_{21}$ and $E_{12}Y_{10}$ are investigated, which were synthesized by sequential anionic polymerization of EOBC[23−25] and EOBCy monomers containing cyanobiphenyl mesogens as shown in Figure 1a, where E denotes the EOBC block and Y denotes the EOBCy block, and the number represents that of repeat units in the component blocks, respectively. The details of the synthesis and chemical characterization are described in the Supporting Information.

As reported previously, EOBC homopolymer exhibits a phase sequence of g-4.6 °C-High Order (HO)-73.4 °C-Smectic A (SmA)-134 °C-I.[23,24] EOBCy homopolymer exhibits a glass transition at 21 °C and a distinct phase transition at 116 °C, as shown in the DSC thermogram in Figure 1b, which is ascribed to nematic-to-isotropic (N−I) transition[26] and confirmed by wide-angle X-ray scattering (WAXS) experiment (Figure S4). For $E_{26}Y_{21}$, only one phase transition located at 130 °C is discernible. Its heat of fusion is 8.2 J/g, which is a sum of that of

Received: July 27, 2014
Accepted: August 26, 2014
Published: August 27, 2014

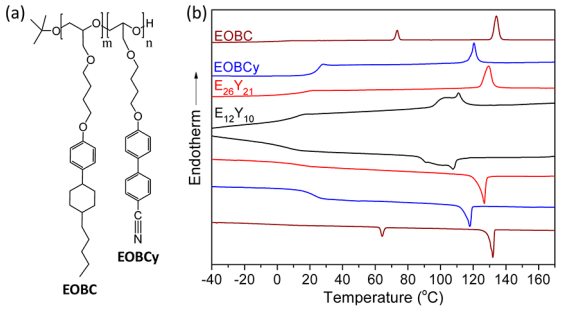

Figure 1. (a) Chemical structure of EOBC-*b*-EOBCy; (b) DSC cooling and subsequent heating thermograms of $E_{26}Y_{21}$ (MW = 16.7 kg/mol), $E_{12}Y_{10}$ (MW = 8.4 kg/mol), EOBCy (MW = 9.3 kg/mol), and EOBC (MW = 13.6 kg/mol) homopolymers at a scanning rate of 10 °C/min.

SmA-I transition of EOBC (12.8 J/g) and N−I transition of EOBCy (2.0 J/g) homopolymers after their compositions taken account (calcd value is 8.3 J/g). This suggests that this transition should encompass isotropization of both blocks, as further confirmed by the following phase structure studies. In contrast, broad, reversible transitions are observed for $E_{12}Y_{10}$ in the temperature range between 84 and 112 °C during heating and cooling processes. The overall heat of fusion 8.6 J/g (calcd value based on composition is 8.2 J/g) is larger than that of either component block. This indicates a coexistence of phase transformations and occurrence of more complex phase behavior, as also discussed below. The HO-SmA transition at 60 °C in EOBC homopolymer[20] can be hardly observed in the copolymers, suggesting the tendency of disruption of hexagonal mesogenic packing within the LC layers in this case.

The evolution of the phase structure of $E_{26}Y_{21}$ is further clarified by temperature-dependent X-ray characterization in accordance to the DSC thermogram. Figure 2 is the small-angle

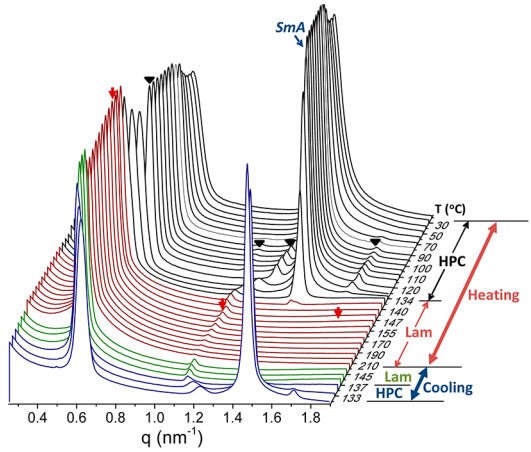

Figure 2. Temperature-dependent SAXS profiles of $E_{26}Y_{21}$ during heating and cooling process.

X-ray scattering (SAXS) profiles of $E_{26}Y_{12}$ in heating and subsequent cooling process. Apparent microphase separated structures are observed and no order-to-disorder transition (ODT) takes place up to 250 °C. This can be ascribed to the huge polarity difference between the chemical structures of these two types of mesogenic groups, which leads to strong incompatibility between the EOBC and EOBCy blocks. The microphase separated structure below 130 °C is identified as a HPC structure, with characteristic scattering peak positions (triangular symbols) at a ratio of q/q^* = 1, $\sqrt{3}$, 2 and $\sqrt{7}$, where q^* = 0.56 nm^{-1} is the location of the lowest-order reflection. The reflection peak located at 1.43 nm^{-1} is attributed to the smectic layers of EOBC block, consistent with that of homopolymer.[20] The scattering from EOBCy block can be identified in the 2D WAXS pattern of the sheared sample, as shown in Figure 3a, where scattering from both smectic and

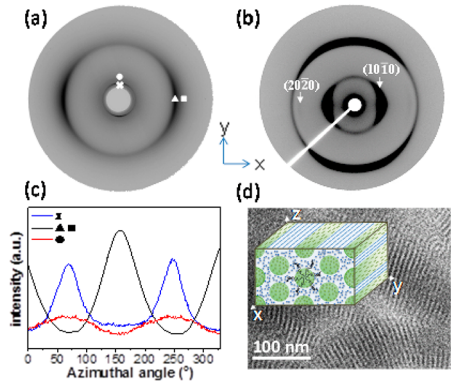

Figure 3. (a) 2D WAXS pattern and (b) 2D SAXS pattern of sheared $E_{26}Y_{21}$ sample along shear gradient (z) direction; (c) Azimuthal scans of radial regions of different symbols in pattern (a), as discussed in the text; (d) TEM image of $E_{26}Y_{21}$ and the inset is the schematic hierarchical order of HPC.

nematic phases can be clearly observed (also illustrated in 1D profile in Figures S8 and S9). The weak scatterings located at 4.75 nm^{-1} (marked as dot symbol), close to diffraction of the third order from smectic layers of EOBC block in the meridian (cross symbol), are ascribed to the short-range position order of nematics in EOBCy block along their director. In the equator, scatterings from mesogenic packing of smectic and nematic orders (marked as triangular and rectangle symbols, respectively) can be identified, which orientation is along the normal of smectic layers as illustrated by the azimuthal scans (Figure 3c). The most probable distances among the mesogens of EOBC and EOBCy blocks are 4.9 and 4.5 Å, respectively, consistent with those of homopolymers (Figure S4).[23,24] In the 2D SAXS pattern (Figure 3b) of the sheared sample, (10$\bar{1}$0) and (20$\bar{2}$0) reflections from HPC are observed on the equator, while those from the smectic layers are located on the meridian. Based on above geometric relationship, we can deduce that mesogens of both blocks align along the axial direction of the cylinders. Considering the volume fraction (ϕ_{EOBCy} = 38%), the cylinders are constituted by EOBCy blocks. The TEM image of the microtomed sample majorly shows parallel cylinders in a diameter of ~7 nm, where EOBCy domains appear light as shown in Figure 3d. This is consistent with the SAXS results. The hierarchical order in the HPC structure is depicted in the inset of Figures 3d and S10.

When the temperature exceeds the isotropization point of the LC phase at 130 °C, OOT from HPC to Lam microstructure (q/q^* = 1, 2, 3, as indicated by arrows) is observed, accompanying with disappearance of characteristic diffraction of the SmA phase, as shown in Figure 2. This process is highly reversible during cooling process. The OOT from Lam to HPC with decrease of temperature is rather unusual. In fact, an increase of the interaction parameter between two blocks with decreasing temperature usually leads

dx.doi.org/10.1021/mz500460j | ACS Macro Lett. 2014, 3, 892−895

to a reversed phase sequence.[2,8,27] This phenomenon cannot be attributed to the change of volume fraction of the blocks when passing through the LC phase transformation either, since EOBC and EOBCy homopolymers are found to exhibit a similar temperature dependence of density up to 160 °C, as shown in Figure S11. Therefore, this exceptional OOT should be directly associated with the unique properties of the S−N diblock copolymer, specifically, the coexistence of nematic and smectic phases, as Lam usually can be stabilized by smectics.[7,8] When OOT occurs, the feature size of the EOBC and EOBCy domains in HPC and Lam changes accordingly, as derived from the SAXS results and their volume fractions. In Lam where EOBC and EOBCy blocks are both in the isotropic state, the thickness of EOBCy layer is 4.1 nm and that of EOBC layer is 7.1 nm. After transition into HPC, the diameter of cylinders of nematic EOBCy becomes 6.8 nm and the center-to-center distance among the cylinders is 10.7 nm with EOBC blocks filled in-between (Figure S10). The apparent shrinkage of EOBC domain through SmA-I transition is consistent with the dielectric results of EOBC homopolymer that the end-to-end distance of the polymer chain indeed decreases after the phase transformation from the isotropic melt to the SmA phase.[24] The fact that the nematic EOBCy chain has to stretch in the cylinder compared to its melt state in Lam agrees with the constraint imposed from the concaved geometry of cylinder. We think that this unusual OOT transition should originate from the LC field induced geometry asymmetry of these two blocks on nanoscale, including the possible effect of the mesogenic packing distance difference (~9%) in nematic and smectic orders which may swell and bend the interface differently.

The S−N diblock copolymer $E_{12}Y_{10}$ has a similar volume composition (ϕ_{EOBCy} = 39%) but nearly half N compared to that of $E_{26}Y_{21}$. This discrepancy leads to dramatically different phase behavior, as already suggested in the DSC measurement. The coexistence of smectics and nematics below the transition temperature (90 °C) has been further implied by WAXD measurements in Supporting Information (Figures S12 and S13). In the X-ray scattering profile of $E_{12}Y_{10}$ (Figure 4a), it can be seen that besides the characteristic scattering peaks from the smectic phase, the rest five diffraction peaks locate at relative position ratios of $\sqrt{3}$, $\sqrt{4}$, $\sqrt{7}$, $\sqrt{13}$, $\sqrt{19}$, corresponding to (211), (220), (321), (510)/(431), and (611)/(532) planes in *Ia*3*d* symmetry ($q_{(211)}$ = 1.05 nm^{-1}). This character indicates the formation of an OBDG structure with lattice constant a = 14.4 nm, in contrast to HPC of $E_{26}Y_{21}$ in the double LC state. This extremely small feature size of the block copolymer benefits from the intrinsic immiscibility between the LC phases.[22]

The evolution of the phase structure of $E_{12}Y_{10}$ is investigated by temperature-dependent SAXS experiment accordingly. As shown in Figure 4b, the OBDG structure remains up to the LC phase transition temperature (~90 °C). When the temperature exceeds 90 °C, the reflection peak belonging to smectic layers in the EOBC block (q_{smA} = 1.58 nm^{-1}) gradually decreases, while the reflections of OBDG get narrower and stronger, suggesting the formation of a more ordered structure. Interestingly, when the temperature rises above 103 °C, the reflection of smectic order starts to develop again; meanwhile, the OBDG structure fades out and finally disappears at 108 °C. Simultaneously, a Lam microstructure in a periodicity of 5.7 nm emerges with two new reflection peaks at a q/q^*_{lam} ratio of 1:2 (q^*_{lam} = 1.09 nm^{-1}). Above 110 °C, the smectic phase starts to

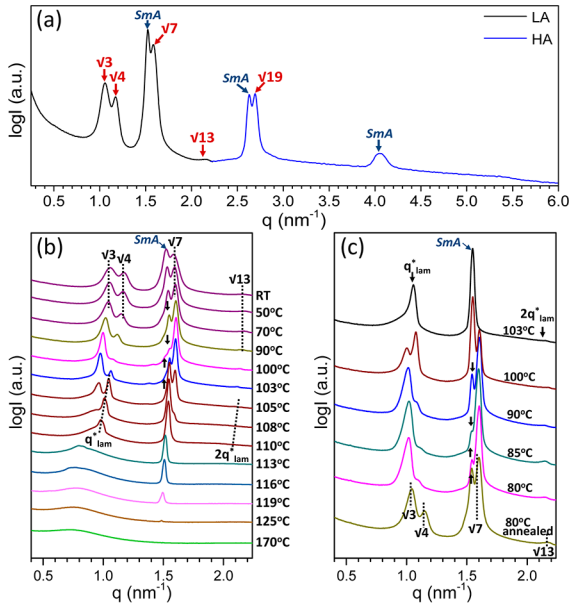

Figure 4. (a) X-ray scattering profiles of $E_{12}Y_{10}$ in low-angle (LA) and high-angle (HA) regions at 25 °C; Temperature-dependent SAXS profiles in heating (b) and cooling (c) processes.

melt, the Lam turns into disordered state eventually. This process is also thermoreversible. As shown in the SAXS profiles in the cooling process (Figure 4c), gradual development of OBDG from Lam is observed when the temperature decreases further below 103 °C. The OBDG structure is well-developed after annealing at 80 °C for 4 h, despite that the smectic order is not as high as that in Lam. This experiment suggests that the OBDG is indeed a thermodynamically stable structure. TEM image of the microtomed sample (Figure 5) displays a network

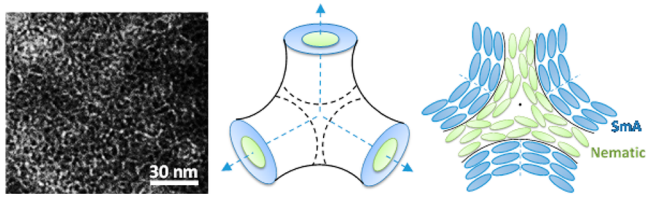

Figure 5. TEM image and schematics of hypothetic LC orderings in OBDG structure.

morphology, characteristic of a bicontinuous structure. Detailed TEM images are also illustrated in Figure S14. The cubic symmetry of the OBDG structure is further supported by the optical measurement, which exhibits almost zero birefringence indicative of an optically isotropic structure (Figure S15).

This interesting phenomenon must be associated with the nature of this class of S−N double LC diblock copolymer. As also implied by temperature-dependent 1D WAXD experiment (Figure S13), the phase transformation starts with partial melting of the smectic phase. This is rather unexpected since the SmA−I transition temperature of EOBC homopolymer is ~20 °C higher than the N−I transition temperature of EOBCy homopolymer. However, this is understandable if considering the highly curvaceous geometry of OBDG structure. In this structure, the nematic EOBCy blocks construct the interweaving network which is composed of tubes and nodes, with each node formed by the intersection of three tubes as schematically shown in Figure 5. The smectic EOBC block fills the rest space

dx.doi.org/10.1021/mz500460j | *ACS Macro Lett.* 2014, 3, 892−895

of the cubic lattice. In general, smectic order is incompatible with cubic symmetry. Tremendous frustration and distortion are thus anticipated in this triply periodic lattice, which would destabilize the smectic order, consequently, resulting in its partial melting at a rather lower temperature. It is worth mentioning that the gyroid structure appears stabilized in the presence of the nematic field, although distortion of nematic field at the center of the connectors is also anticipated. Further melting of nematics makes the gyroid structure no longer stable. Thereafter, smectic order is regained and transformation into Lam is induced. After the melting of the smectic phase, the sample gets into a disordered state. The decrease of ODT temperature of $E_{12}Y_{10}$ is consistent with the decrease of χN (χ is the Flory−Huggins interaction parameter) due to the smaller N. The intermediate degree of segregation usually leads to a gyroid phase.[2]

How the symmetries of the LC phases would accommodate this morphological geometry is a sufficiently complicated puzzle. The peculiarity of this OBDG superstructure with coexistence of smectic and nematic orders reminds us the highly frustrated as well as extremely fantastical blue phase of chiral nematics, whose cubic phase is thought to be stabilized by a regular lattice of disclination defects in a periodicity on the order of visible light wavelength.[28] Whereas, the cubic lattice of the S−N diblock copolymer, free of molecular chirality, is on the nanometer scale in contrast. Although tremendous topological defects such as disclinations are unavoidable, they have to be readily accommodated in this nanometer-sized cubic lattice. Our experimental work sets out new theoretical challenges to understand the relationship between geometrical frustration and LC order.

In summary, our work demonstrates a remarkable alliances of frustration and order in the S−N double LC block copolymers. This unique combination and variable composition drive the new discovery of diverse and complex hierarchical structures and are expected to meet the central challenge of programming complexity of soft matter. It also potentially opens up the possibilities in creating novel, functional materials in future, such as patterned structure on the sub-10 nm scale.

■ ASSOCIATED CONTENT

Supporting Information

Details of synthesis and characterization. This material is available free of charge via the Internet at http://pubs.acs.org.

■ AUTHOR INFORMATION

Corresponding Author

*E-mail: hmxiong@sjtu.edu.cn.

Notes

The authors declare no competing financial interest.

■ ACKNOWLEDGMENTS

We appreciate BL14B and BL16B beamlines in SSRF. Research is supported by the NSFC (No. 21074070) and NCET-11-0335.

■ REFERENCES

(1) Bates, F. S.; Fredrickson, G. H. *Annu. Rev. Phys. Chem.* **1990**, *41*, 525.

(2) Hamley, I. W. *The Physics of Block Copolymers*; Oxford University Press: Oxford, U.K., 1998.

(3) Zhu, L.; Cheng, S. Z. D.; Calhoun, B. H.; Ge, Q.; Quirk, R. P.; Thomas, E. L.; Hsiao, B. S.; Yeh, F.; Lotz, B. *J. Am. Chem. Soc.* **2000**, *122*, 5957.

(4) Loo, Y. L.; Register, R. A.; Ryan, A. J. *J. Am. Chem. Soc.* **2002**, *35*, 2365.

(5) Muthukumar, M.; Ober, C. K.; Thomas, E. L. *Science* **1997**, *227*, 1225.

(6) Sänger, J.; Gronski, W.; Maas, S.; Stühn, B.; Heck, B. *Macromolecules* **1997**, *30*, 6783.

(7) Schneider, A.; Zanna, J. J.; Yamada, M.; Finkelmann, H.; Thomann, R. *Macromolecules* **2000**, *33*, 639.

(8) Anthamatten, M.; Hammond, P. T. *J. Polym. Sci., Part B: Polym. Phys.* **2001**, *39*, 2671.

(9) Tenneti, K. K.; Chen, X. F.; Li, C. Y.; Tu, Y. F.; Wan, X. H.; Zhou, Q. F.; Sics, I.; Hsiao, B. S. *J. Am. Chem. Soc.* **2005**, *127*, 15481.

(10) Zhao, Y.; Qi, B.; Tong, X.; Zhao, Y. *Macromolecules* **2008**, *41*, 3823.

(11) Zhu, Y. F.; Guan, X. L.; Shen, Z. H.; Fan, X. H.; Zhou, Q. F. *Macromolecules* **2012**, *45*, 3346.

(12) Fukuhara, K.; Fujii, Y.; Nagashima, Y.; Hara, M.; Nagano, S.; Seki, T. *Angew. Chem., Int. Ed.* **2013**, *52*, 5988.

(13) Ruokolainen, J.; Mäkinen, R.; Torkkeli, M.; Mäkelä, T.; Serimaa, R.; ten Brinke, G.; Ikkala, O. *Science* **1998**, *280*, 557.

(14) Aida, T.; E. Meijer, W.; Stupp, S. I. *Science* **2012**, *335*, 813.

(15) Li, J.; Kamata, K.; Watanabe, S.; Iyoda, T. *Adv. Mater.* **2007**, *19*, 1267.

(16) Ikeda, T.; Mamiya, J.; Yu, Y. L. *Angew. Chem., Int. Ed.* **2007**, *46*, 506.

(17) Mabrouk, E.; Cuvelier, D.; Brochard-Wyart, F.; Nassoy, P.; Li, M. H. *Proc. Natl. Acad. Sci. U.S.A.* **2009**, *106*, 18.

(18) Patel, S. N.; Javier, A. E.; Beers, K. M.; Pople, J. A.; Ho, V.; Segalman, R. A.; Balsara, N. P. *Nano Lett.* **2012**, *12*, 4901.

(19) Thurn-Albrecht, T.; Schotter, J.; Kastle, G. A.; Emley, N.; Shibauchi, T.; Krusin-Elbaum, L.; Guarini, K.; Black, C. T.; Tuominen, M. T.; Russell, T. P. *Science* **2000**, *290*, 2126.

(20) Tang, C. B.; Lennon, E. M.; Fredrickson, G. H.; Kramer, E. J.; Hawker, C. J. *Science* **2008**, *322*, 429.

(21) Bates, C. M.; Maher, M. J.; Janes, D. W.; Ellison, C. J.; Willson, C. G. *Macromolecules* **2014**, *47*, 2.

(22) Dierking, I. *Textures of Liquid Crystals*; Wiley-VCH Verlag GmbH & Co. KGaA: Weinheim, 2003; p 167.

(23) Liu, Y.; Wei, W.; Xiong, H. M. *Polymer* **2013**, *54*, 6572.

(24) Liu, Y.; Li, Y. G.; Xiong, H. M. *ACS Macro Lett.* **2013**, *2*, 45.

(25) Wei, W.; Liu, Y.; Xiong, H. M. *Polymer* **2013**, *54*, 6793.

(26) Montornes, J. M.; Reina, J. A.; Ronda, J. C. *J. Polym. Sci., Part A: Polym. Chem.* **2004**, *42*, 3002.

(27) Khandpur, A. K.; Foerster, S.; Bates, F. S.; Hamley, I. W.; Ryan, A. J.; Bars, W.; Almdal, K.; Montensen, K. *Macromolecules* **1995**, *28*, 8796.

(28) de Gennes, P. G.; Prost, J. *The Physics of Liquid Crystals*, 2nd ed.; Oxford University Press: New York, 1995.